# RSC Advances

# Journal Name

## ARTICLE

# Selective removal of thiosulfate from thiocyanate-containing water by a three-dimensional structured adsorbent-calcined NiAl-layered double hydroxide film

Xiaohua Liu, Weiliang Tian, Xianggui Kong, Meihong Jiang, Xiaoming Sun, Xiaodong Lei*

NiAl-layered double hydroxide (NiAl-LDH) platelets were uniformly grown on porous Ni foam substrate by a facile *in situ* hydrothermal method. By subsequent calcination, the three-dimensional (3D) structured adsorbent, calcined NiAl-layered double hydroxide film/Ni foam (NiAl-LDO/NF) was obtained. Batch experiments were carried out to investigate the selective adsorption performance of the obtained material for thiosulfate and thiocyanate anions in water, compared with the powder NiAl-LDO adsorbent. The results show that the NiAl-LDO/NF has highly selective adsorption for $S_2O_3^{2-}$ in the mixture solution with a maximum adsorptive capacity about 209.4 mg/g at room temperature, while the removal capacity for $SCN^-$ was only about 15.9 mg/g. At the same time, the resulted 3D structured adsorbent exhibited higher preferential adsorption and easier separation performance from the solution than the corresponding NiAl-LDO powder. It was found that the adsorbability and selectivity of this material was maintained well after more than 10 regeneration cycles. Therefore, the obtained 3D hierarchical NiAl-LDO/NF can be considered as potential structured adsorbent in environmental applications for selective removal of $S_2O_3^{2-}$ from $SCN^-$-containing aqueous solution.

## Introduction

As reported, sulfur-contaminated wastewater endangers the living of creatures and should be responsible for the environmental deterioration in some ways. Sulfur-containing pollutants bring severe hazardous influence on the aquatic organisms and ecosystem when the sulfur-effluents released without proper treatment, for the presence of sulfuric anions (sulfate, thiosulfate, thiocyanate, etc.) would inhibit the function of enzymes in organisms and lower the pH value of corresponding aqueous solutions.[1,2] Meanwhile, the cycle and effective utilization of sulfur resource are global significant and have been received considerable attention.[3] Sulfur-containing anions always co-exist in wastewaters delivered from diverse industrial processes including coking, photo finishing, textile manufacturing, electroplating, dyeing, and mining.[2,4–8] The effective separation of thiocyanate and thiosulfate has potentially industrial application and commercial value, because both thiocyanate and thiosulfate play important role in pharmaceutical and agro-industry, respectively.[9–11] While it was difficult to separate the two anions by traditional methods, such as the resource wasting, high-cost and low efficiency of electrodialysis, ion exchange, wet-oxidation and biodegradation.[1,6,12–16] Adsorption is believed to be a feasible and efficient approach for pollutant removal from

contaminated solutions.[17–22] However, the post-processing and regeneration of powder adsorbents are challenges remained to achieve greater economical accessibility in practical applications.

The layered double hydroxides (LDHs), which could be represented by the general formula $[M^{2+}_{1-x} M^{3+}_x (OH)_2]^{x+} (A^{n-})_{x/n} \cdot yH_2O$, where $M^{2+}$ represents a divalent metal cation, $M^{3+}$ a trivalent metal cation, $A^{n-}$ an anion, x ranges from 0.15 to 0.33 for pure LDH formation, and y is typically of the order 1–2.[23-29] In the past decades, LDHs with characteristic lamellar structure, specific anion exchange property and large surface area (about 20–120 $m^2$/g ), have attracted highly attention in various fields such as catalysis,[23] electrical materials,[24] light-emitting materials,[25] and adsorption.[26,27] And the products obtained from calcination of LDH precursors at about 400–500 °C,[28,29] have been widely used as adsorbents for the removal of anionic contaminants, such as $SCN^-$,[16,19] $PO_4^{3-}$,[30] boron,[31] Cr(VI),[32] acid dye,[33] etc. In the previous work, our group have successfully separated $S_2O_3^{2-}$ and $SCN^-$ anions (the ratio of $[S_2O_3^{2-}]$ and $[SCN^-]$ has been changed from 1:1 to 1:7 )[11] by using calcined MgAl-LDH powder as adsorbent. However, the restraining factors for comprehensive application of LDO powder adsorbents are obvious: the aggregation of adsorbent particles, laborious separation in post-processing, difficulties in recycling process. Therefore, some researchers have focused on the fabrication and application of monolithic structured adsorbents with controllable morphology and mechanical stability.[34]

*State Key Laboratory of Chemical Resource Engineering, Beijing University of Chemical Technology, PO Box 98, Beijing 100029, China. E-mail: leixd@mail.buct.edu.cn; Fax: +86-10-64425385; Tel: +86-10-64455357*

The porous foam metals as a style of materials integrated function and construction performance, have attracted much attention in both industrial separation process and electrochemical application.[35–37] The cross−linked network endows the structural materials with high geometric surface areas and low mass transportation resistance.[38,39] LDH films with hierarchical architectures have been successfully prepared on foam metal substrates by in−situ crystallization technique and sol−gel nano−copying process, which showed fascinating performances to remove organic and inorganic pollutants in water treatment.[40,41] The network substrates consisted of interconnected channels and macro−pores are beneficial for the dispersion and fixation of LDH flakes, which further improved the mechanical stability as well as the avoidance of aggregation.

In this work, the as−prepared NiAl−LDO/NF was used as structured adsorbent for selective adsorption of $S_2O_3^{2-}$ from SCN$^-$−containing wastewater. At the same time, we investigated the adsorption−regeneration of the structured adsorbent during the selective adsorption process. Moreover, the structured NiAl−LDO/NF adsorbent with high selective adsorption capacity, good reusability and fine solid−liquid separability was proved to be a promising material in water treatment for the selective separation of different anionic pollutants.

## Experimental section

### Materials

Nickel foams (purity: 99.5%) were purchased from Kunshan Desi Electronic Technology Co., Ltd. The other analytical grade chemicals, including $Ni(NO_3)_2 \cdot 6H_2O$, $Al(NO_3)_3 \cdot 9H_2O$, urea, NaSCN and $Na_2S_2O_3$ were obtained from Beijing Chemical Reagent Company and used without further purification.

### Synthesis of structured and powder adsorbents

Nickel foams (30 mm × 40 mm × 1 mm, weight 0.517 g) with 3D network were used as the substrates of structured adsorbent. They were degreased in ethanol for 10 min, ultrasonically cleaned in 3 mol/L hydrochloride acid for 10 min, washed by deionized water for 3 times, then dried at 60 °C at $N_2$ atmosphere in an oven. After pretreatment, a piece of dried nickel foam was vertically immersed into 80 mL aqueous solution of $Ni(NO_3)_2 \cdot 6H_2O$ (0.009 mol), $Al(NO_3)_3 \cdot 9H_2O$ (0.003 mol) and urea (0.054 mol) that dissolved in deionized water. This mixture was sealed in a 100 mL Teflon-lined autoclave and maintained at 120 °C for 12 h. The prepared NiAl−LDH film on nickel foam (denoted as NiAl−LDH/NF) was washed three times with deionized water and dried at 60 °C for 10 h. After calcined at 400 °C for 3 h with a heating rate of 5 °C /min, the final structured adsorbent (denoted as NiAl−LDO/NF) was obtained by cooling the sample. The powder NiAl−LDH sample was prepared by coprecipitation method with the same conditions, without nickel foam added into the reaction vessel.

### Batch selective adsorption tests

To investigate the selective adsorption behavior of NiAl−LDO/NF, batch adsorption tests were carried out in 200 mL of glass vessels on magnetic stirring apparatus. The initial concentration of $S_2O_3^{2-}$, equal to that of SCN$^-$ ranged from 0.05 to 0.5 mmol/L in 100 mL SCN$^-$−containing solution. One piece of NiAl−LDO/NF (with a size of 30 mm×40 mm×1 mm) was suspended in the solution stirred with an agitation speed of 100 rpm at 25 ± 2 °C for 240 min. Four hour was found to be enough to reach adsorption equilibrium. During the adsorption process, ca. 2 mL solution was taken out by syringe and filtered by 0.22 μm organic membrane filter at regular intervals. The concentrations of $S_2O_3^{2-}$ and SCN$^-$ in the filtrate were measured by an ion chromatography instrument (Dionex ICS−90A, USA) with an AS 25 column (Dionex, USA) and a conductivity detector. The mobile phase was sodium hydroxide solution (36 mmol/L) at a flow rate of 0.9 mL/min. For comparison with the powder samples and pure Ni foam substrate, controlled experiments were performed under the same conditions except the adsorbents. The pure substrate, with the same size as the as−prepared NiAl−LDO/NF, was calcined at 400 °C before immersed into the solution.

The adsorption capacity ($Q_e$) and removal percentage (R %) of $S_2O_3^{2-}$ and SCN$^-$ can be calculated by the following equations:

$$Q_e = \frac{V \cdot (C_0 - C_e)}{m} \quad (1)$$

$$R(\%) = \frac{C_0 - C_e}{C_0} \times 100\% \quad (2)$$

Where $Q_e$ (mg/g) is the equilibrium adsorption capacity, $C_0$ and $C_e$ (mg/L) mean the initial and equilibrium concentration of corresponding anions. V (L) and m (g) represent the volume of solution and the mass of adsorbent, respectively. R (%) is the removal percentage of anions.

### Desorption and regeneration tests

After the adsorption process reached equilibrium, the structured adsorbent was taken out from the sulfur−containing solution and washed with deionized water to remove any un−adsorbed thiosulfate and thiocyanate anions. The desorption of $S_2O_3^{2-}$ from the structured adsorbent was carried out by dipping the samples in a 100 mL 0.02 mol/L of $Na_2CO_3$ solution with continuous stirring for 6 h in air at room temperature. The anions exchanged NiAl−LDH/NF was rinsed thoroughly by deionized water for three times, calcined at 400 °C for 3 h. Then, the regenerated structure adsorbent was immersed into mixed $S_2O_3^{2-}$ and SCN$^-$ aqueous solution with the same concentrations of in the first adsorption process. This procedure on adsorption−regeneration cycle was repeated 10 times. The concentration of residual $S_2O_3^{2-}$ and SCN$^-$ after each adsorption cycle was detected by the same ion chromatography method.

### Characterization

**Fig. 1** XRD patterns of (a) the Ni foam substrate, (b) NiAl−LDH/NF, (c) NiAl−LDH powder prepared by coprecipitation, (d) NiAl−LDO powder scraped from NiAl−LDO/NF and (e) NiAl−LDO/NF.
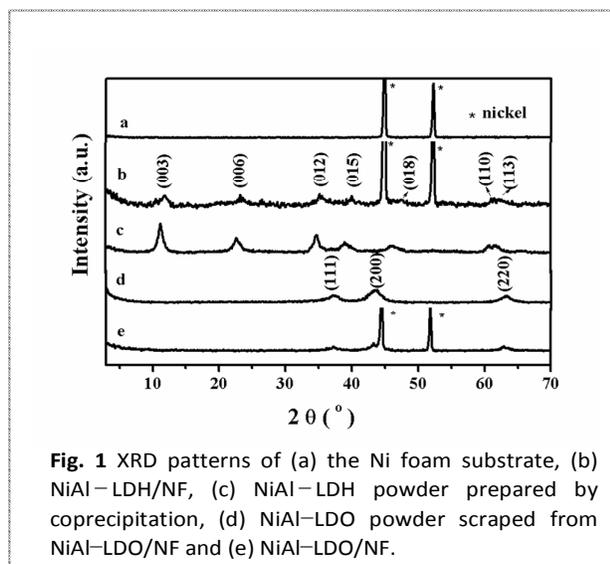
The powder X−ray diffraction (XRD) patterns of the samples were recorded on a Shimadzu XRD−6000 diffractometer with Cu Kα radiation (λ = 0.15418 nm, 40 kV, 30 mA) in the 2θ range of 3−70° with a scanning rate of 10° min$^{-1}$. Fourier transform infrared (FTIR) spectra were collected using the KBr pellet technique (sample : KBr = 1 : 100, mg/mg) on a Bruker Vector 22 Fourier transform spectrometer in the range of 4000 − 400 cm$^{-1}$ with a resolution of 2 cm$^{-1}$. Scanning electron microscope (SEM) images were obtained by using a Hitachi S4700 apparatus with the applied voltage of 20 kV. To avoid charging effect, the surface of samples were covered with a thin platinum layer after spray−platinum treatment. The elemental analysis for metal ions of adsorbents was performed on an Oxford Link−Isis 300 Energy Dispersive X−ray spectroscopy (EDX). Inductively coupled plasma atomic emission spectroscopy (ICPS−7500) was also used to indirectly measure the loaded capacity of LDH or LDO on the substrate. Solutions were prepared by dissolving a small amount of powder samples that scraped from the NiAl−LDH/NF or NiAl-LDO/NF in dilute HNO$_3$ solution. The low-temperature N$_2$ adsorption-desorption experiments were carried out using a Quantachrome Autosorb-1 system. Samples were outgassed at 373 K for 8 h. The specific surface areas were calculated using the Brunauer-Emmett-Teller (BET) method based on the N$_2$ adsorption isotherms.

## Results and discussion

### Structure and morphology of as−prepared NiAl−LDO/NF and its precursor

The XRD patterns of NiAl−LDH/NF and NiAl−LDO/NF samples are shown in Fig. 1. Two sharp diffraction peaks of Ni at 44.9° and 52.4° (JCPDS Card No: 04−0850) superimposed on the broad feature due to the substrate (Fig. 1a), are observed in the case of the NiAl−LDH/NF sample (Fig. 1b). Comparison of the XRD patterns of powder scraped from the NiAl−LDH/NF sample (Fig. 1c), JCPDS card No: 15 − 0087, and the



**Fig. 2** FTIR spectra of (a) NiAl−LDH powder and (b) NiAl−LDO powder scraped from the nickel foam substrate, respectively.
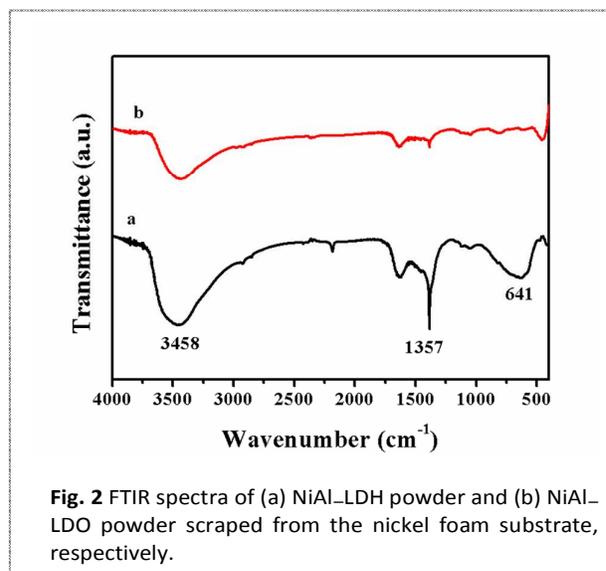
literatures[42,43] show that the low angle peaks correspond to the basal reflection of CO$_3^{2-}$−containing NiAl−LDH (d$_{003}$ = 0.78 nm). The other peaks can be indexed as the (006), (012), (015), (018), (110) and (113) reflections of an LDH phase. For NiAl−LDO/NF (Fig. 1d), we can also find that the peaks of Ni superimposed on the XRD pattern of NiAl−LDO powder scraped from NiAl−LDO/NF sample (Fig. 1d). After calcined at 400 °C, the two LDO samples exhibit the characteristic peaks of poorly crystalline NiO structure (Fig.s 1d and 1e) in accordance with reports in the literature.[44] Compared with that of NiAl−LDH/NF (Fig. 1b) and NiAl−LDO/NF (Fig. 1e), the disappearance of characteristic (00l) reflections for LDH phase and the presence of typical reflections of (111), (200), (220) planes for NiO phase (JCPDS NO. 65−2901)[45] indicates the LDH phase was almost disappeared after 3 h of calcination at 400 °C in air. FTIR spectra of NiAl−LDH powder and NiAl−LDO powder scraped from the nickel foam substrate respectively are shown



**Fig. 3** SEM images of as-prepared NiAl−LDH/NF (a) at low magnification and (b) high magnification, (c) side view and (d) top view of NiAl−LDO/NF at high magnification (Insets: (a) pristine Ni foam substrate and (b) EDX of NiAl−LDH/NF surface).
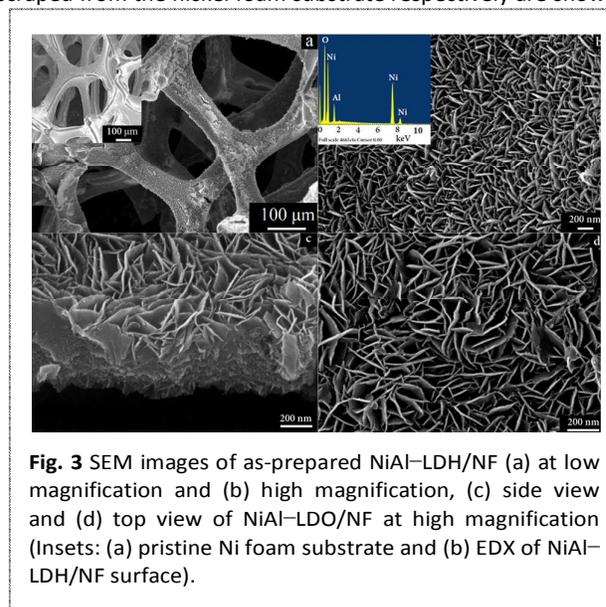
in Fig. 2. In Fig. 2a, the broad band between 3700−3000 cm$^{-1}$ is assigned to the stretching vibrations of O−H groups in the brucite−like layers of LDH phase. The adsorption band at ca. 1357 cm$^{-1}$ in the spectrum of NiAl−LDH powder is attributed to the characteristic stretching vibration of $CO_3^{2-}$ groups, which was consistent with XRD analysis. The NiAl−LDO sample obtained after calcination (Fig. 2b) shows the disappearance of absorption band at 1357 cm$^{-1}$ for carbonate, which indicates that the interlayer carbonate was delaminated by the calcination process.

The growth of NiAl−LDH platelets on the 3D nickel foam substrate was based on the precipitation from homogeneous solutions using the hydrolysis of urea at 120 °C, which leads to an increase in concentration of $CO_3^{2-}$ and pH (the latter associated with the formation of ammonia), resulting in crystallized NiAl−LDH platelets. Nickel foam has a 3D network structure (inset of Fig. 3a), which greatly increases the surface area of substrate. Fig. 3a and b display the morphology of the NiAl−LDH film on the nickel foam substrate. It can be seen that the NiAl−LDH platelets have grown on the nickel foam and that, in general, the (00l) planes of NiAl−LDH platelets were almost perpendicular to the surface of the Ni foam and each platelet has a hexagonal shape (Fig. 3b). However, the NiAl−LDH particles are chemically immobilized throughout the Ni foam substrate. Through the EDX spectrum of the NiAl−LDH/NF surface (inset of Fig. 3b), it can be calculated that the Ni/Al molar ratio was about 2.9, which approximates to the original addition molar ratio of Ni/Al (about 3.0). NiAl−LDO/NF was obtained after the process of thermal decomposition of NiAl−LDH/NF at 400 °C to remove the interlayer $CO_3^{2-}$. As shown in the Fig. 3c and d, the NiAl−LDO film layer retained the staggered sheet morphology of NiAl−LDH and an open−pore structure. This is mainly a response to the dehydration, dehydroxylation and $CO_3^{2-}$ delamination carried out in the process of thermal decomposition. It was found that the NiAl−LDO platelets were not detached from the Ni foam after calcination. Fig. 3c is the cross section image of the NiAl−LDO/NF. It also found that the NiAl−LDO film was attached on the substrate tightly, there is only one platelet layer of NiAl−LDO on the surface and the thickness of the NiAl−LDO layer was about 300 nm. We found that the whole
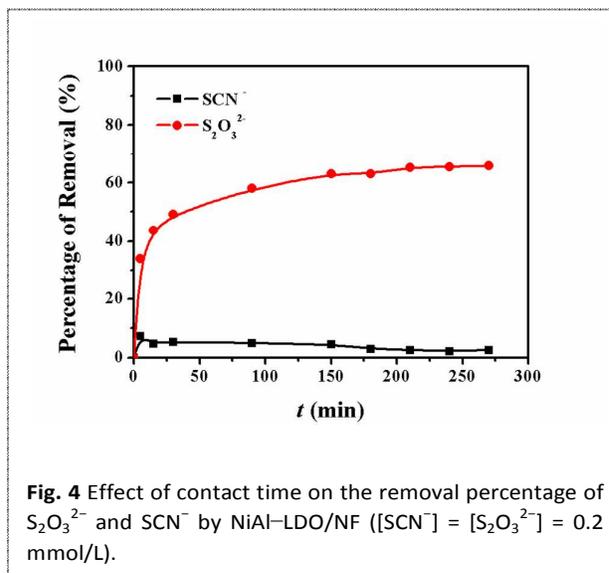


**Fig. 4** Effect of contact time on the removal percentage of $S_2O_3^{2-}$ and SCN$^-$ by NiAl−LDO/NF ([SCN$^-$] = [$S_2O_3^{2-}$] = 0.2 mmol/L).

weight of obtained NiAl−LDH/NF (ca. 0.467 g, 30 mm × 40 mm × 1 mm) was slightly lighter than that of the pure nickel foam (ca. 0.517 g), which could be attributed to a little Ni dissolved in the alkaline ammonium solution. Therefore, the load of NiAl−LDH on the Ni foam cannot directly calculated by weighing the difference of obtained NiAl−LDH/NF and the initial substrate. The weight percentage of NiAl−LDH grown on Ni foam was calculated to be approximately 3.34 wt% by the results of ICP measurement for the amounts of Ni and Al elements (the Ni element resourced from the substrate has been considered). The loss weight was about 0.33 g per gram of NiAl−LDH when NiAl−LDH was calcined to NiAl−LDO. Therefore, the weight percentage of active component NiAl−LDO on the structured adsorbent was about 2.44 wt%. According the low-temperature $N_2$ adsorption-desorption experiments, the specific areas of pure Ni foam, NiAl-LDO/NF and NiAl-LDO powder are 21.8, 27.1 and 92.9 m$^2$/g, respectively. By deducted the Ni foam, the specific area of NiAl-LDO on NiAl-LDO/NF was ca. 121.1 m$^2$/g. It is found that the specific area of NiAl-LDO on NiAl-LDO/NF was higher than that of NiAl-LDO powder, obviously, which is beneficial to improve the adsorption performance of NiAl-LDO.



**Fig. 5** Effect of initial concentration on the adsorption of (a) $S_2O_3^{2-}$ and (b) SCN$^-$ by NiAl−LDO/NF ([SCN$^-$] = [ $S_2O_3^{2-}$], adsorption time was 240 min).
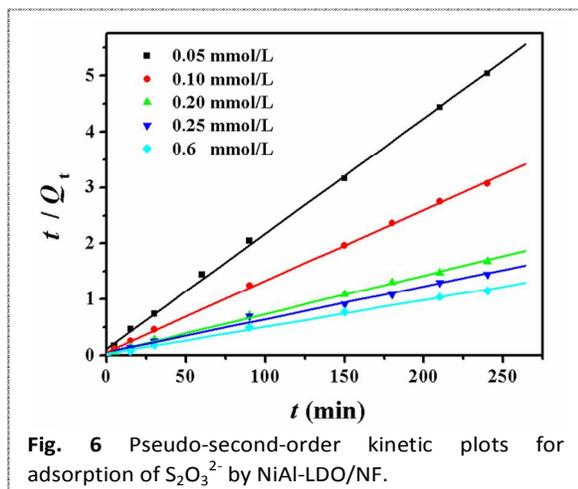
**Fig. 6** Pseudo-second-order kinetic plots for adsorption of $S_2O_3^{2-}$ by NiAl-LDO/NF.



**Fig. 8** The effect of initial pH on the selective removal of $S_2O_3^{2-}$ and $SCN^-$ by NiAl-LDO/NF.

### Selective adsorption behavior of NiAl−LDO/NF

The selective adsorption ability of the structured adsorbent NiAl−LDO/NF from the mixed aqueous solution was studied with adsorption time and initial concentrations of anions. The adsorption curves shown in Fig. 4 and 5, both the results show that NiAl−LDO/NF is able to preferentially remove $S_2O_3^{2-}$ from the $SCN^-$−containing solution. From Fig. 4, we can see when one piece of NiAl−LDO/NF was set in the solution, the removal percentage of $S_2O_3^{2-}$ by NiAl−LDO/NF was always much higher than that of $SCN^-$. When the initial concentration of $SCN^-$ and $S_2O_3^{2-}$ were 0.2 mmol/L respectively, the removal percentage ratio was $[S_2O_3^{2-}]$ : $[SCN^-]$ = 65.4% : 2.1% after adsorption for 240 min. The high preferential adsorption of NiAl−LDO/NF for $S_2O_3^{2-}$ over $SCN^-$ can be attributed to the higher charge density of $S_2O_3^{2-}$ anions, leading to stronger affinity between them and the positive layers of the NiAl−LDH host.[46] After 180 min of selective adsorption by the structured adsorbent, the residual $SCN^-$ in the mixture had a concentration 2.8 times that of $S_2O_3^{2-}$. Additionally, the residual concentration ratio of $[SCN^-]$ : $[S_2O_3^{2-}]$ can be substantially increased by adding more pieces



**Fig. 7** Adsorption curves of $S_2O_3^{2-}$ and $SCN^-$ vs time using NiAl−LDO/NF, NiAl−LDO powder and pure Ni foam as absorbents in the mixed solution of $S_2O_3^{2-}$ and $SCN^-$ ($[SCN^-]$ = $[S_2O_3^{2-}]$ = 0.05 mmol/L).

of NiAl−LDO/NF, which would be beneficial to obtain high quality thiocyanate by subsequent crystallization.

The initial concentrations of anions in the $SCN^-$−containing solution also influenced the selective adsorption performance, as shown in Fig. 5 for a piece of NiAl−LDO/NF and varying (but equimolar) concentrations of $S_2O_3^{2-}$ and $SCN^-$. At low concentration, $[S_2O_3^{2-}]$ = $[SCN^-]$ = 0.05 mmol/L, the removal of $S_2O_3^{2-}$ reached about 79.9% despite the adsorption capacity ($Q_e$) was only about 47.3 mg/g (Fig. 5a), the removal of $SCN^-$ was only about 5.1% and the $Q_e$ was ca. 1.2 mg/g (Fig. 5b), which resulted in a $[SCN^-]$ : $[S_2O_3^{2-}]$ ratio in the remaining solution of about 4.7 : 1. When the concentrations of $SCN^-$ and $S_2O_3^{2-}$ in the mixed solution were increased, both the removal percentage of $SCN^-$ and $S_2O_3^{2-}$ decreased. When the concentrations of anions were increased to 0.6 mmol/L, the removal percentage of $S_2O_3^{2-}$ was fell to only about 15.8% with a very high $Q_e$ (ca. 209.4 mg/g), but the removal percentage of $SCN^-$ fell to only about 1.6% and the $Q_e$ was about 15.9 mg/g. However, it was proved that the resulting structured adsorbent NiAl−LDO/NF shows a good selective adsorption of $S_2O_3^{2-}$ in $SCN^-$−containing solution.

The kinetics of $S_2O_3^{2-}$ removal at various initial concentrations, as an important characteristic to define the adsorption efficiency, was studied to understand the adsorption behavior of the as-prepared structured adsorbent NiAl-LDO/NF (Fig. 6). The kinetics of $SCN^-$ removal cannot be given because of the influence of the selective $S_2O_3^{2-}$

**Table1.** Kinetic parameters for the adsorption of $S_2O_3^{2-}$ by NiAl-LDO/NF based on the pseudo-second-order Model.

| $C_0$ mmol/L | $Q_{e,exp}$ mg/g | $k_2$ g/(mg·min) | $Q_{e,cal}$ mg/g | $R^2$ |
|---|---|---|---|---|
| 0.05 | 47.3 | 0.003772 | 48.5 | 0.9994 |
| 0.10 | 78.1 | 0.003005 | 78.6 | 0.9997 |
| 0.20 | 143.4 | 0.001026 | 144.7 | 0.9991 |
| 0.25 | 165.4 | 0.000590 | 170.4 | 0.9958 |
| 0.60 | 209.4 | 0.000880 | 207.9 | 0.9984 |

**Table 2.** Comparison of the Langmuir and Freundlich model parameters

| Adsorbent | Langmuir | | | Freundlich | | |
|---|---|---|---|---|---|---|
| | $Q_{max}$ (mg/g) | $K_L$ (L/mg) | $R^2$ | n | $K_F$ (L/g) | $R^2$ |
| NiAl-LDO/NF | 229.4 | 0.1895 | 0.9993 | 2.47 | 49.934 | 0.8865 |

adsorption. Among the kinetic models tested, pseudo-second-order kinetic (eq. 3) gave a satisfactory description of $S_2O_3^{2-}$ removal by NiAl-LDO/NF with high correlation coefficients ($R^2$ > 0.99).

$$\frac{t}{Q_t} = \frac{1}{k_2 Q_e^2} + \frac{t}{Q_e}$$
(3)

Where $Q_e$ and $Q_t$ are the capacity of adsorbate (mg/g) on the NiAl-LDO/NF at equilibrium and time t (min), respectively; $k_2$ (g/(mg·min)) is the pseudo-second-order kinetic rate constant. According to the slope and intercept of lines presented in Fig. 6, the kinetic parameters were calculated and listed in Table 1. The experimental amount ($Q_{e,exp}$) of $S_2O_3^{2-}$ adsorbed by NiAl-LDO/NF matches well with the calculated one ($Q_{e,cal}$) on the basis of pseudo-second-order kinetic model. A decreased tendency of rate constant $k_2$ can be seen in the Table 1, with the increasing of initial concentration. The pseudo-second order equation is based on the uptake capacity of the solid phase and is in agreement with a chemisorption mechanism being the rate determining step. Another advantage of the pseudo-second order model is that it predicted the behavior over the whole range of the adsorption process.[2]

The equilibrium of thiosulfate separated between liquid and solid phase were analyzed by two general-purpose adsorption



**Fig. 9** Photographs of $S_2O_3^{2-}$ and SCN$^-$ mixed solution in the presence of NiAl−LDO/NF (a and b) and NiAl−LDO powder (c and d) adsorbents during adsorption process and at the end of the experiments.

isotherm models: Langmuir (eq. 4) and Freundlich model (eq. 5). The parameters were listed in Table 2. As is shown, the equilibrium isotherm is typically following the Langmuir model, judging from the correlation coefficients. The Langmuir isotherm is applicable to a homogeneous surface where all potential adsorption sites have equal affinity for the guest.[48]

$$\frac{C_e}{Q_e} = \frac{1}{Q_{max} K_L} + \frac{C_e}{Q_{max}}$$
(4)

$$\ln Q_e = \ln K_L + \frac{1}{n} \ln C_e$$
(5)

For comparison purpose, the selective adsorption performances of NiAl-LDO/NF, NiAl–LDO powder and pure Ni foam in the SCN$^-$ and $S_2O_3^{2-}$ mixed solution are shown in Fig. 6. The dosage of NiAl–LDO powder was 0.011 g, accounting for about 2.44 wt % of a piece of NiAl–LDO/NF (about 0.451 g) used in the controlled experiment. The size of pure Ni foam was the same as NiAl–LDO/NF (30 mm × 40 mm × 1 mm). From Fig. 7, it is revealed that there was a little removal for $S_2O_3^{2-}$ and SCN$^-$ by pristine Ni foam. With an adsorption duration of 240 min, for the structured NiAl–LDO/NF adsorbent, the removal percentage of $S_2O_3^{2-}$ reached ca. 80.1 %, whereas the removal of SCN$^-$ was 5.1 %. But for NiAl–LDO powder adsorbent, it was about 38.9 % for $S_2O_3^{2-}$ and 9.5 % for SCN$^-$. Obviously, the removal of $S_2O_3^{2-}$ by structured NiAl−LDO/NF is higher than that of NiAl–LDO powder and the removal of SCN$^-$ by NiAl–LDO/NF is lower than that of NiAl–LDO powder, suggesting that the selectivity of $S_2O_3^{2-}$ with NiAl−LDO powder was not as good as that of structured NiAl−LDO/NF, though both of them could realize a successful separation of these mixed pollutants. The results unambiguously indicated that the network Ni foam substrate consisted of interconnected channels and macro−pores with high geometric surface area improved the dispersion as well as the avoidance of aggregation of NiAl−LDO flakes. At the same time, there is a lower mass transportation resistance for 3D structured NiAl−LDO/NF during the adsorption process than that of NiAl−LDO powder. We also investigated the influence of initial pH of mixed solution on the selective adsorption. As is shown in Fig. 8, in the pH range from 5 to 11, there is no obvious change for the selective adsorption for $S_2O_3^{2-}$ and SCN$^-$ on the structured NiAl−LDO/NF.

The great advantage of using such a structured adsorbent was the avoidance of adsorbent−water separation which is generally encountered with liquid−phase adsorptions and the high adsorbate−active phase contact surface due to the structure and size of adsorbent. From Fig. 9, the adsorption processes can be visually observed by using NiAl−LDO/NF and NiAl−LDO powder as adsorbents. The result
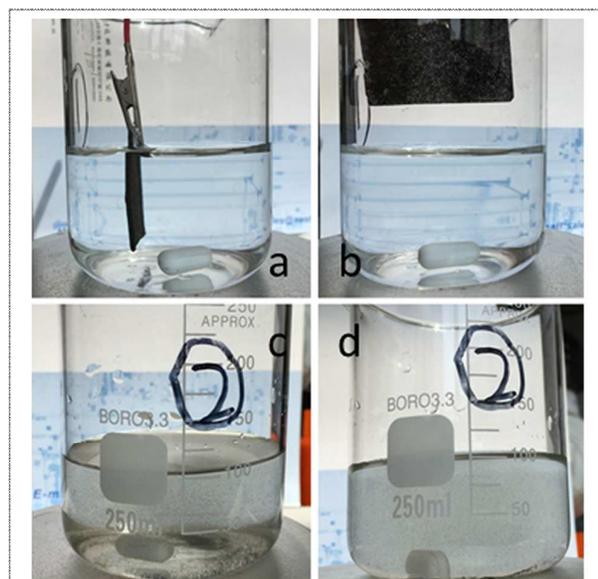
*RSC Advances Accepted Manuscript*

demonstrated that the structured NiAl−LDO/NF could be easily separated from the solution (Fig. 9a and b) compared with the powder adsorbent (Fig. 9c and d). In addition, during the adsorption process with violent stirring, no NiAl−LDO particle was found exfoliating from NiAl−LDO/NF to the solution, suggesting that NiAl − LDO/NF is a mechanically stable structured adsorbent with favorable selective adsorbability for $S_2O_3^{2-}$ in SCN−containing solution.

### Regeneration and recycling of NiAl−LDO/NF

The development of an efficient and low−cost regeneration method for adsorbents is economically important.[47] By anion−exchanging, $S_2O_3^{2-}$ desorption from the used NiAl−LDO/NF was carried out in a $Na_2CO_3$ solution. It is easy for $CO_3^{2-}$ replacing the adsorbed $S_2O_3^{2-}$ owing to the high affinity of $CO_3^{2-}$ with the layers of LDH materials than that of $S_2O_3^{2-}$.[48] By subsequently calcining, the structured NiAl−LDO/NF was reconverted as selective adsorption material for reuse. Consecutive adsorption−regeneration cycles for SCN− and $S_2O_3^{2-}$ mixed solution with the NiAl−LDO/NF adsorbent were repeated 10 times under the same experimental conditions. Fig. 10 shows that at the first regeneration cycle of the structured adsorbent, $S_2O_3^{2-}$ removal percentage has more than 80% and the adsorption of SCN− was hardly observed. In addition, the removal percentage of $S_2O_3^{2-}$ by NiAl−LDO/NF diminishes progressively with each cycle of regeneration and that of SCN− was still lower than 6.0%. The outstanding adsorption−regeneration performance of the NiAl−LDO/NF is related to the 3D hierarchical structure which facilitates a high dispersion of NiAl−LDO platelets. Moreover, after the first adsorption−regeneration (Fig. 11a) and 10 consecutive cycles of adsorption−regeneration (Fig. 11b), there are some tiny changes in its morphology were observed: the surface of the latter turned into roughness and some cracks appeared because of calcinations. These changes may be caused by thermal expansion and contraction of Ni foam during anion−exchange and calcination process, which resulted in slight loss of NiAl−LDO particles from Ni foam substrate and reduced the removal percentage of $S_2O_3^{2-}$. However, at the last cycle, the



**Fig. 11** SEM images of NiAl−LDO/NF after the first adsorption−regeneration (a) and 10 consecutive cycles of adsorption−regeneration (b).

structured adsorbent still has more than 51% of the $S_2O_3^{2-}$ removal percentage and maintained very high selectivity.

## Conclusions

A 3D hierarchical NiAl−LDH/NF has been prepared by in−situ hydrothermal growth method used urea as precipitant. By subsequent calcination, the as−prepared NiAl−LDO/NF was good structured adsorbent for the preferential removal of $S_2O_3^{2-}$ from a mixed aqueous solution of $S_2O_3^{2-}$ and SCN−. $S_2O_3^{2-}$ was adsorbed by the structured material, and SCN− was left in the solution. The adsorption capacity of $S_2O_3^{2-}$ can reached about 209.4 mg/g while only about 15.9 mg/g for SCN−. Furthermore, the structured NiAl−LDO/NF can be easily separated from the mixed solution with high mechanical stability during the selective adsorption process. Adsorption−regeneration cycle study demonstrated that the structured adsorbent can be regenerated and reused at least 10 times. It can be concluded that the as−prepared 3D hierarchical NiAl−LDO/NF is an efficient and potential structured adsorbent with highly selective adsorbability and reusability in the resourcing of industrial $S_2O_3^{2-}$ and SCN− mixed effluent.

**Fig. 10** Recycling experiment with 10 consecutive cycles of adsorption-regeneration by NiAl−LDO/NF ([SCN−] = [ $S_2O_3^{2-}$ ] = 0.05 mmol/L).

## Notes and references

1    N. Dizge, E. Demirbas and M. Kobya, *J. Hazard. Mater.*, 2009, **166**, 1367-1376.
2    C. Geng, T. Xu, Y. Li, Chang, X. Sun and X. Lei, *Chem. Eng. J.*, 2013, **232**, 510-518.
3    D. T. Johnston, B. C. Gill, A. Masterson, E. Beirne, K. L. Casciotti, A. N. Knapp and W. Berelson, *Nature*, 2014, **513**, 530-533.
4    J. Vicente and M. Diaz, *Environ. Sci. Technol.*, 2003, **37**, 1452-1456.
5    N. Yin, G. Yang, Z. Zhong and W. Xing, *Desalination*, 2011, **268**, 233-237.
6    P. Oulego, S. Collado, L. Garrido, A. Laca, M. Rendueles and M. Diaz, *J. Environ. Manage.*, 2014, **132**, 16-23.
7    C. Namasivayam and M. V. Sureshkumar, *Process Saf. Environ. Prot.*, 2007, **85**, 521-525.
8    O. N. Kononova, A. G. Kholmogorov, N. V. Danilenko, N. G. Goryaeva, K. A. Shatnykh and S. V. Kachin, *Hydrometallurgy*, 2007, **88**, 189-195.
9    Y. J. Kim and J. H. Choi, *Water Res.*, 2012, **46**, 6033-6039.
10   H. Sharghi, M. A. Nasseri and A. H. Nejad, *J. Mol. Catal., A*, 2003, **206**, 53-57.
11   X. Yu, Z. Chang, X. Sun, X. Lei, D. G. Evans, S. Xu and F. Zhang, *Chem. Eng. J.*, 2011, **169**, 151-156.
12   S. Collado, A. Laca and M. Diaz, *J. Hazard. Mater.*, 2010, **177**, 183-189.
13   M. B. Stotta, P. D. Franzmann, L. R. Zappia, H. R. Watling, L. P. Quan, B. J. Clark, M. R. Houchin, P. C. Miller and T. L. Williams, *Hydrometallurgy*, 2001, **62**, 93-105.
14   C. Namasivayam and K. Prathap, *J. Environ. Eng. Manage.*, 2006, **16**, 267-274.
15   C. Staib and P. Lant, *Biochem. Eng. J.*, 2007, **34**, 122-130.
16   T. Wu, D. Sun, Y. Li, H. Zhang and F. Lu, *J. Colloid Interface Sci.*, 2011, **355**, 198-203.
17   Y. Zou, M. Vera and A. E. Rodrigues, *Sep. Purif. Technol.*, 2002, **26**, 195–205.
18   L. Lv, J. He, M. Wei, D. G. Evans and X. Duan, *Water Res.*, 2006, **40**, 735-743.
19   Y. Li, B. Gao, T. Wu, W. Chen, X. Li and B. Wang, *Colloids Surf., A*, 2008, **325**, 38-43.
20   Y. Zou and A. E. Rodrigues, *Energy Convers. Manage.*, 2002, **43**, 1865-1876.
21   Y. Li, B. Gao, T. Wu, D. Sun, X. Li, B. Wang and F. Lu, *Water Res.*, 2009, **43**, 3067-3075.
22   E. Ayranci and B. E. Conway, *Anal. Chem.*, 2001, **73**, 1181-1189. .
23   P. J. Sideris, U. G. Nielsen, Z. Gan and C. P. Grey, *Science*, 2008, **321**, 113-117.
24   V. Nicolosi, M. Chhowalla, M. G. Kanatzidis, M. S. Strano and J. N. oleman, *Science*, 2013, **340**, 1420.
25   M. Liu, T. Wang, H. Ma, Y. Fu, K. Hu and C. Guan, *Sci. Rep.*, 2014, **4**, 7147.
26   L. Zhong, J. Hu, A. Cao, Q. Liu, W. Song and L. Wan, *Chem. Mater.*, 2007, **19**, 1648-1655 .
27   J. Fei, Y. Cui, X. Yan, W. Qi, Y. Yang, K. Wang, Q. He and J. Li, *Adv. Mater.*, 2008, **20**, 452-456.
28   L. Lv, J. He, M. Wei, D. G. Evans and X. Duan, *J. Hazard. Mater.*, 2006, **133**, 119-128.
29   D. Carriazo, M. del Arco, C. Martín and V. Rives, *Appl. Clay Sci.*, 2007, **37**, 231-239.
30   J. Das, B. S. Patra, N. Baliarsingh and K. M. Parida, *Appl. Clay Sci.*, 2006, **32**, 252-260.
31   L. Kentjono, J. Liu, W. Chang and C. Irawan, *Desalination*, 2010, **262**, 280-283.
32   Z. Zhang, M. Liao, H. Zeng, S. Xu, X. Liu, J. Du, P. Zhu and Q. Huang, *Appl. Clay Sci.*, 2014, **102**, 246-253.
33   F. Jiao, L. Shuai, J. Yu, X. Jiang, X. Chen and S. Du, *Trans. Nonferr. Metal. Soc. China*, 2014, **24**, 3971-3978.
34   L. Zhong, J. Hu, H. Liang, A. Cao, W. Song and L. Wan, *Adv. Mater.*, 2006, **18**, 2426-2431.
35   Y. Wang, Y. Zhao, C. Xu, D. Zhao, M. Xu, Z. Su and H. Li, *J. Power Sources*, 2010, **195**, 6496-6499.
36   G. Yang, C. Xu and H. Li, *Chem. Commun.*, 2008, 6537-6539.
37   B. Wang, G. R. Williams, Z. Chang, M. Jiang, J. Liu, X. Lei and X. Sun, *ACS Appl. Mater. Interf.*, 2014, **6**, 16304-16311.
38   O. Sanz, F. Javier Echave, M. Sánchez, A. Monzón and M. Montes, *Appl. Catal., A*, 2008, **340**, 125-132.
39   M. A. Leon, R. Tschentscher, T. A. Nijhuis, J. van der Schaaf and J. C. Schouten, *Ind. Eng. Chem. Res.*, 2011, **50**, 3184-3193.
40   S. He, Y. Zhao, M. Wei, D. G. Evans and X. Duan, *Ind. Eng. Chem. Res.*, 2012, **51**, 285-291.
41   Y. Zhao, S. He, M. Wei, D. G. Evans and X. Duan, *Chem. Commun.*, 2010, **46**, 3031-3033.
42   B. Wang, Q. Liu, Z. Qian, X. Zhang, J. Wang, Z. Li, H. Yan, Z. Gao, F. Zhao and L. Liu, *J. Power Sources*, 2014, **246**, 747-753.
43   Z. Gao, J. Wang, Z. Li, W. Yang, B. Wang, M. Hou, Y. He, Q. Liu, T. Mann, P. Yang, M. Zhang and L. Liu, *Chem. Mater.*, 2011, **23**, 3509-3516.
44   M. Wei, X. Xu, X. Wang, F. Li, H. Zhang, Y. Lu, M. Pu, D. G. Evans and X. Duan, *Eur. J. Inorg. Chem.*, 2006, 2831-2838.
45   Z. Liang, R. Huo, Y. Yin, F. Zhang, S. Xu and Y. Guo, *Electrochim. Acta*, 2013, **108**, 429-434.
46   D. G. Evans and X. Duan, *Chem. Commun.*, 2006, **5**, 485-496.
47   K. H. Goh, T. T. Lim and Z. Dong, *Water Res.*, 2008, **42**, 1343-1368.
48   X. Lei, M. Jin and G. R. Williams, *Energy Environ. Focus*, 2014, **3**, 4-22.